Received 10 November 2015; revised 25 January 2016; accepted 29 January 2016. Date of publication 8 February 2016; date of current version 22 April 2016.
The review of this paper was arranged by Editor C. C. McAndrew.

Digital Object Identifier 10.1109/JEDS.2016.2527045

Phase Noise Reduction in a VHF MEMS-CMOS Oscillator Using Phononic Crystals

PEI QIN, HAOSHEN ZHU (Student Member, IEEE), JOSHUA E.-Y. LEE (Member, IEEE), QUAN XUE (Fellow, IEEE)

Department of Electronic Engineering and State Key Laboratory of Millimeter Waves, City University of Hong Kong, Hong Kong

CORRESPONDING AUTHOR: Q. XUE (e-mail: eeqxue@cityu.edu.hk)

This work was supported in part by the Hong Kong Research Grants Council under Project CityU 116113, in part by the National Basic Research Program of China (973 Program) under Grant 2014CB339900, and in part by the National Natural Science Foundation of China under Grant 61372056.

ABSTRACT This paper presents experimental results showing reduced phase noise in a very high frequency band microelectromechanical systems (MEMS) oscillator. This has been achieved by engineering the embedded MEMS resonator with phononic crystal structures. The aluminum nitride on silicon MEMS resonator with phononic crystal tethers achieves an unloaded quality factor (Q_u) 2.3 times of the same resonator with a simple tether design. The increase in Q_u leads to a measured 6dB close-to-carrier phase noise reduction in an MEMS-based oscillator that sustained by a transimpedance amplifier implemented in 65nm CMOS process. The 141 MHz MEMS-CMOS oscillator with phononic crystal tethers has a phase noise better than −83dBc/Hz at 1 kHz offset and −134dBc/Hz at the far-from-carrier range while consuming less than 3mW.

INDEX TERMS Microelectromechanical systems (MEMS), oscillator, quality factor, phase noise, phononic crystal.

I. INTRODUCTION

Advances in microfabrication have initiated interest to develop microelectromechanical systems (MEMS) resonators as timing and frequency references [1] in place of traditional quartz crystals. These MEMS resonators not only deliver a more compact size, but also promise to achieve lower cost, higher level of integration and better reliability due to the potential CMOS-compatibility of the fabrication processes and maturity of advanced wafer-level packaging technologies [2]. By leveraging on high quality factor, good power handling capability of bulk-mode silicon resonators and the excellent electromechanical coupling provided by piezoelectric (e.g., AlN) thin-films, Aluminum Nitride on Silicon (AlN-on-Si) MEMS resonators are highly promising for high-frequency low phase noise reference oscillators. While the best AlN-on-Si MEMS oscillators can deliver excellent phase noise floor performance, their close-to-carrier phase noise performance is typically worse than silicon MEMS oscillators owing to their lower quality factor at the same resonant frequency.

The quality factor of MEMS resonators is usually limited by multiple loss factors, including thermoelastic damping, Akhiezer loss, anchor loss, interface loss, air damping among other losses [3]. For AlN-on-Si MEMS resonators, it has been found that anchor loss [4], interface loss [4], [5] and the effect of charge redistribution [6] are major contributors for energy dissipation. To minimize the anchor loss and improve quality factor, approaches using planar acoustic reflectors [7] and phononic crystal structures [8]–[10] have been explored recently. But neither of these approaches has been applied in oscillators for phase noise improvement.

For filters and oscillators, it is also critical that quality factor is enhanced selectively at the desired resonance mode and exclude spurious modes. We have shown such selectivity in the enhancement of quality factor recently based on 1D phononic crystal tethers [11]. In this work, we integrate the 1D phononic crystal resonator with a transimpedance amplifier designed in a 65nm CMOS process to implement a MEMS-CMOS oscillator. We show that phase noise is reduced as a result of employing phononic crystal tethers.

II. DESIGN AND CHARACTERIZATION

The common series-resonant MEMS oscillator topology [12] is adopted here by interfacing the resonators with the

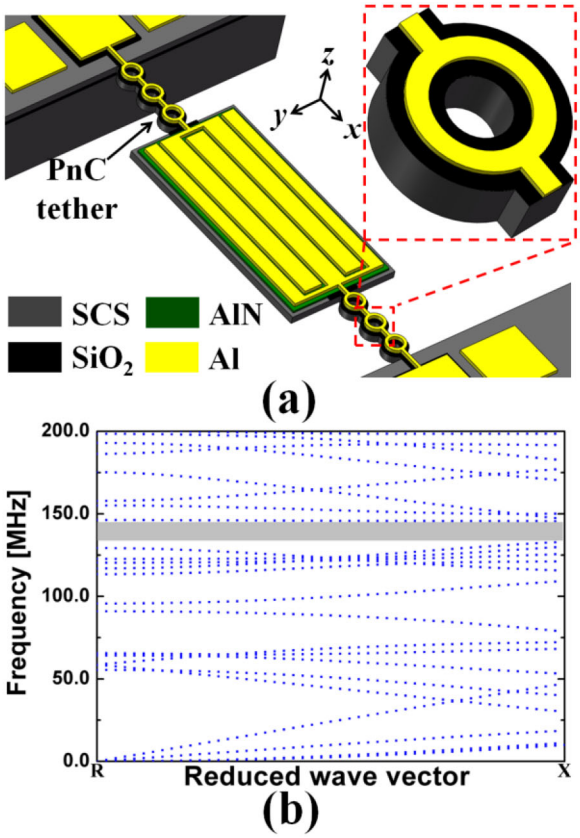

FIGURE 1. (a) Perspective view of the two-port lateral width-extensional mode AlN-on-Si resonator supported by phononic crystal tethers. Inset: magnified view of a phononic crystal unit cell; (b) Simulated acoustic band diagram of the phononic crystal structure. The acoustic bandgap is highlighted as the gray zone.

designed shunt-shunt feedback CMOS transimpedance amplifier.

A. MEMS RESONATOR

As shown in Fig. 1a, the AlN-on-Si resonator supported by phononic crystal tethers was designed to resonate in the width-extensional mode, which delivers high quality factor and good electromechanical coupling [7]. The pitch distance between two adjacent fingers is 30μm and defines the half wavelength (λ/2) of the longitudinal wave appearing in the *y*-direction. According to finite-element simulation, the AlN-on-Si resonator exhibits a ~141MHz resonant frequency for the intended 5th order width-extensional mode when the sides of the resonator lie along the <110> orientation of the single-crystal silicon device layer. Given that the acoustic wavelength is much larger than the silicon layer thickness, the dispersion of longitudinal wave is not significant. The resonant frequency (f) of the width-extensional mode can be roughly estimated as:

$$f = \frac{1}{\lambda}\sqrt{\frac{E}{\rho}}, \tag{1}$$

where E and ρ are the Young's modulus in <110> axes and the density of single-crystal silicon, respectively.

The 1D phononic crystal ring-shape structure shown in the inset of Fig. 1 is known to form acoustic bandgaps which prevent acoustic waves at specified frequency bands from propagating through the structure [9]. When applied as tethers of a resonator, these structures have the effect of blocking acoustic waves in the *x*-direction from leaking to the substrate. This in turn reduces anchor loss. Referring to Fig. 1a, our phononic crystal unit cell has a 200nm SiO_2 isolation layer between the 10μm single-crystal silicon and 1μm Al layers in place of AlN (as used in [8] and [9]) to prevent unwanted actuation on the tethers. By applying Floquet periodicity on the unit cell's two ends, the finite-element simulated band structure (Fig. 1b) indicates a wide acoustic bandgaps (gray zone) in the 133~145MHz range for an infinite 1D phononic crystal strip; the frequency of the desired 5th order mode lies the acoustic bandgaps. While extending the number of phononic crystal cells offers better acoustic isolation in theory, experimentally we have found that quality factor does not improve much beyond 3 cells [6], when other loss factors (i.e., interface loss [4], [5] and the loss due to charge redistribution [6]) start to prevail.

The AlN-on-Si resonators were fabricated using a 5-mask foundry SOI MEMS process, which is detailed in our previous work [10]. The fabricated devices (depicted in Fig. 2) were characterized using microwave probes (Picoprobe Model 40A) in a probe station and a vector network analyzer (Agilent N5230A). A standard two-port setup was adopted and SOLT (short, open, load and through) calibration was performed. The measured electrical transmission (S_{21}) of the resonator with phononic crystal tethers is compared against the one with beam tethers [7], [13] in Fig. 2. For beam tethered resonators, it is common to set the length to be equal to odd multiples of a quarter wavelength (λ/4) to minimize the anchor loss [14]. In our case, the length of the tether was designed to be 3λ/4 (45μm). Besides, the width of straight beam tethers was made to be the same as the width of the ends of phononic crystal tether for fair comparison. Both resonators were measured in air and room temperature (300K). We see that unloaded quality factor (Q_u) is greatly improved from 2600 to 6200 while motional resistance (R_m) is accordingly reduced from 171Ω to 77Ω by replacing the beam tether with the phononic crystal structure. The resulting product of frequency and quality factor of our phononic crystal enhanced device is on par with the best current AlN-on-Si resonators [1].

B. CMOS TRANSIMPEDANCE AMPLIFIER

The transimpedance amplifier circuit topology is shown in Fig. 3a. In the first stage, a tunable shunt-shunt feedback resistor is connected between the input and output nodes of the common source amplifier, performing as the current-to-voltage converter. The second and third stages aim to provide the transimpedance amplifier with sufficient gain and the last stage works for lowering the output impedance. Supplied with V_{DD} of 0.8V, PMOS current source transistors are loaded for all stages to keep higher voltage headroom.

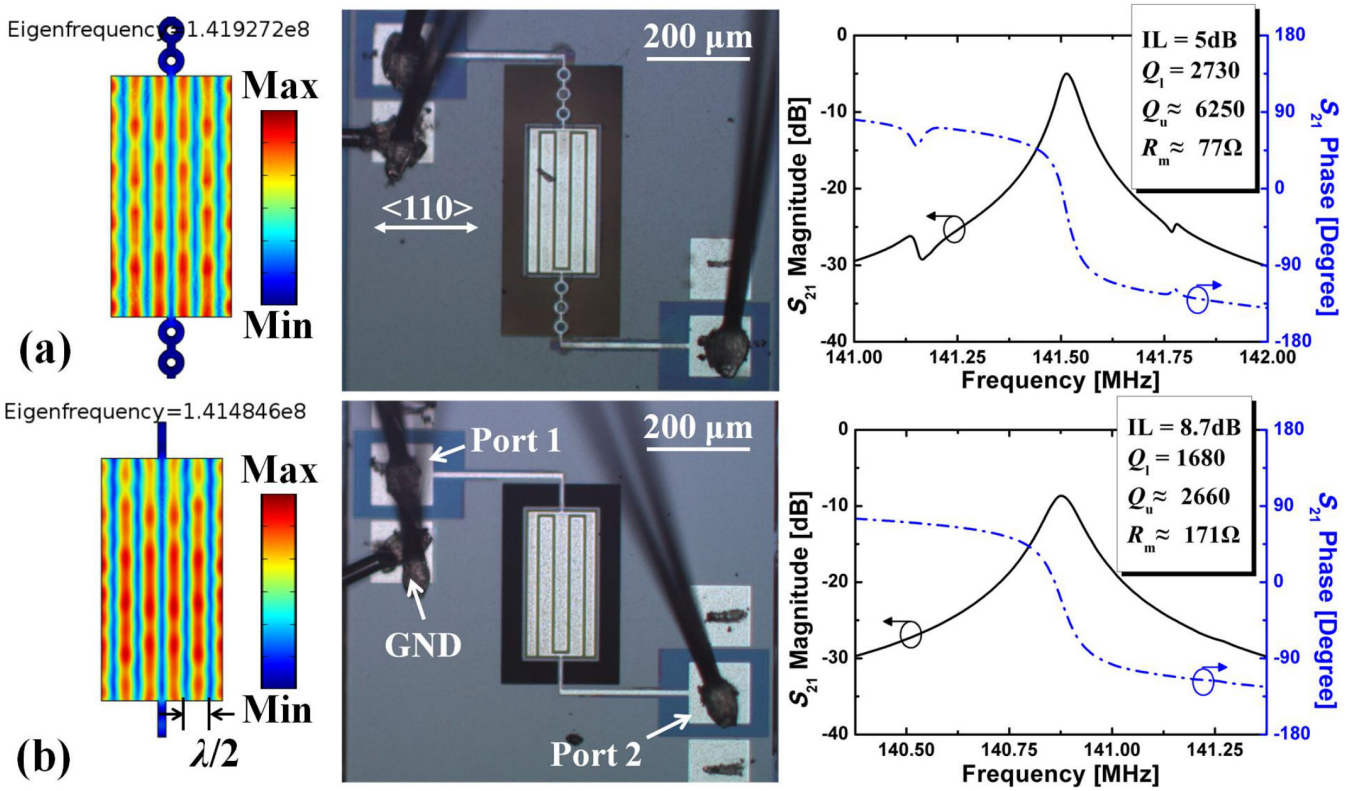

FIGURE 2. **Finite-element simulation of vibration mode shapes, optical micrographs of the fabricated AlN-on-Si resonators supported by (a) phononic crystal tethers (b) beam tethers (i.e., without phononic crystals) and their corresponding transmissions (S_{21}) for the desired 5th-order width-extensional mode. IL: insertion loss; Q_l: the loaded quality factor referring to 50Ω terminations from the vector network analyzer.**

The transimpedance amplifier tends to deliver a total phase shift of 0° to interface the MEMS resonator with nearly 0° phase shift at its series resonance.

The transimpedance amplifier was designed and implemented in the 65nm 1P9M RF CMOS process by TSMC, which has benefits of small footprint, low power consumption and large bandwidth. The layout area of the transimpedance amplifier plus a 50Ω output buffer is 100µm×50µm, representing one of the most compact transimpedance amplifiers for MEMS-based oscillators. The integrated circuit die (Fig. 3b) was wire bonded to a printed circuit board and characterized with vector network analyzer. The measured bandwidth is about 250MHz for a transimpedance gain of 54dBΩ (∼500Ω) (Fig. 3c), which is sufficient for sustaining oscillation for our resonator here. It should be noted that the bandwidth of the transimpedance amplifier is severely lowered by the parasitic capacitance of the bonding wires and printed circuit board. The post-layout simulation indicates that the bandwidth exceeds 950MHz for a 54dBΩ gain and 0.5pF capacitive load.

According to the classical Leeson's model [15], the phase noise of an oscillator can be expressed as:

$$L(f_m) = \frac{2k_B TF}{P_0}\left[1+\left(\frac{f_0}{2Q_l f_m}\right)^2\right]\left(1+\frac{f_\alpha}{f_m}\right) \qquad (2)$$

where f_m is the offset frequency, f_0 is the oscillation frequency, f_α is a constant that relates with flicker noise corner, k_B, P_0, T and F are the Boltzmann constant, carrier power, absolute temperature, and noise factor of the amplifier, respectively. The close-to-carrier phase noise is inversely proportional to Q_l^2, which in general relates to Q_u as follows:

$$Q_l = \frac{R_m}{R_m + R_{in} + R_{out}} Q_u, \qquad (3)$$

where R_{in} and R_{out} are respectively the input and output resistances of the transimpedance amplifier. To accentuate the lowering of phase noise as a result of boosting Q_u, lower R_{in} and R_{out} were realized at the cost of higher power consumption. The transimpedance amplifier consumes 3.6mA from a 0.8V dc supply.

III. OSCILLATOR IMPLEMENTATION AND MEASUREMENTS

The transimpedance amplifier and AlN-on-Si resonators were connected through wire bonds as shown in Fig. 4a. The measured output time-domain waveform and frequency spectrum of the oscillator based on a phononic crystal resonator are shown in Fig. 4b and Fig. 5, respectively. The phase noise of the oscillator was measured using a signal analyzer (Agilent N9030A). Fig. 6 shows that the phononic crystal enhanced oscillator has a better phase noise performance at

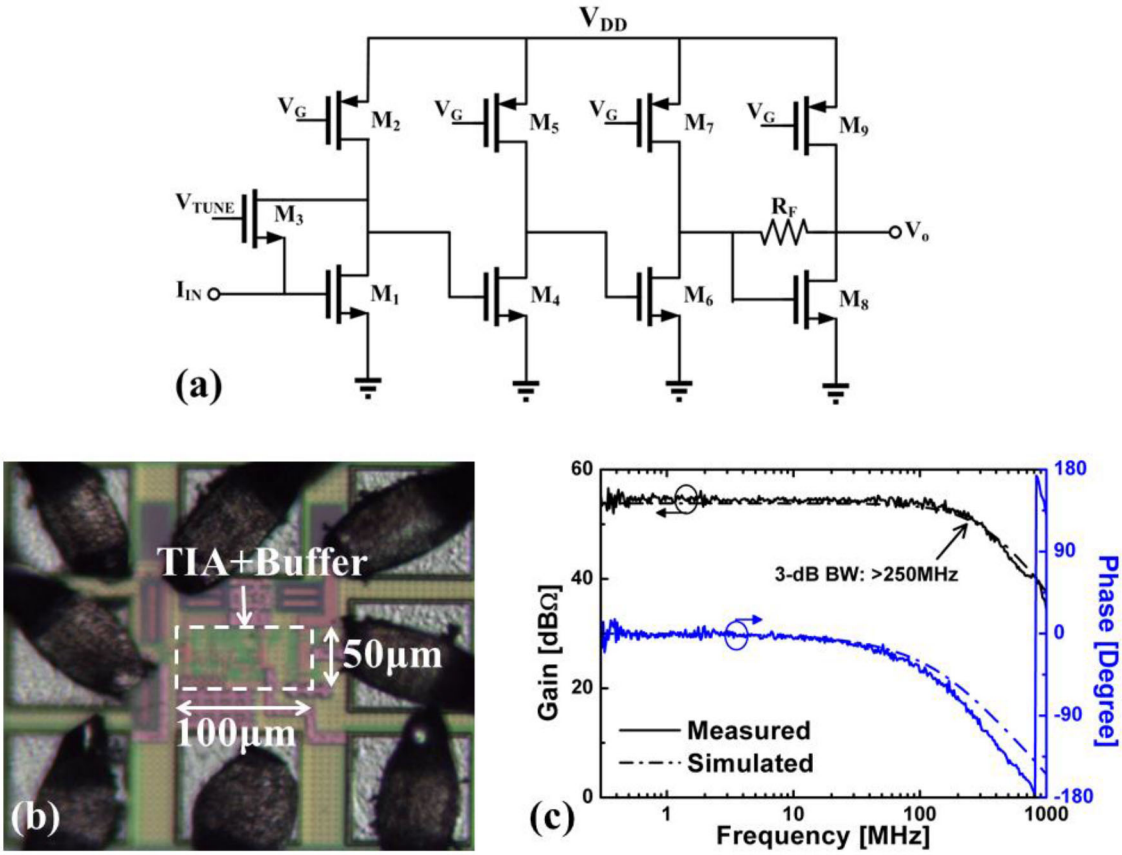

FIGURE 3. **(a) Circuit topology of the CMOS transimpedance amplifier; (b) The optical micrograph of the fabricated CMOS transimpedance amplifier; (c) The measured and simulated transimpedance gain and phase response of the transimpedance amplifier (The simulation is performed with 5pF shunt capacitive load).**

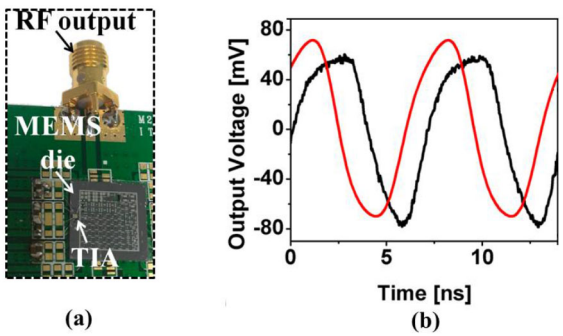

FIGURE 4. **(a) Fabricated MEMS-CMOS oscillator on a printed circuit board, (b) measured (black) and simulated (red) time-domain waveform.**

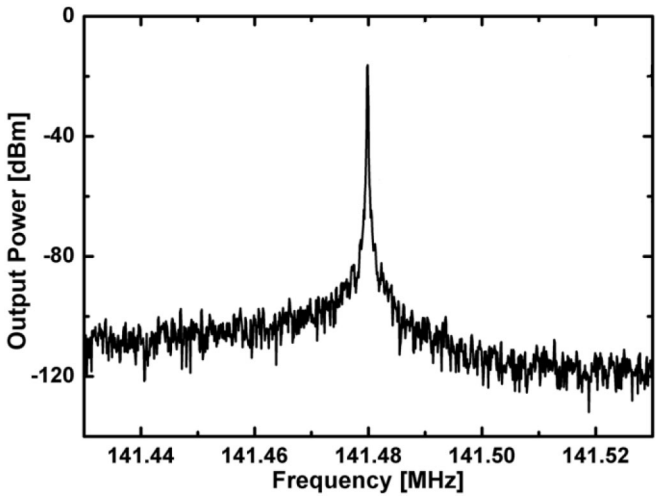

FIGURE 5. **Measured output frequency spectrum of the MEMS oscillator based on the phononic crystal resonator.**

the close-to-carrier range than with a beam tether resonator. Due to relatively low R_{in} and R_{out} of the transimpedance amplifier, the loaded quality factor of the phononic crystal resonator is roughly doubled compared to the beam-tethered device, which corroborates the measured 6dB phase noise reduction at 1kHz offset. Theoretically, the close-to-carrier phase noise could be enhanced up to ~7.2dB for an increase in unloaded quality factor by 2.3 times, which could be achieved by minimizing the electrical loading ($R_{\text{in}} = R_{\text{out}} = 0\Omega$).

To validate the measured phase noise behavior for both oscillators, the electrical behaviors of the AlN-on-Si resonators were modeled as a linear equivalent circuit (as shown in Fig. 7) and co-simulated with the CMOS transimpedance

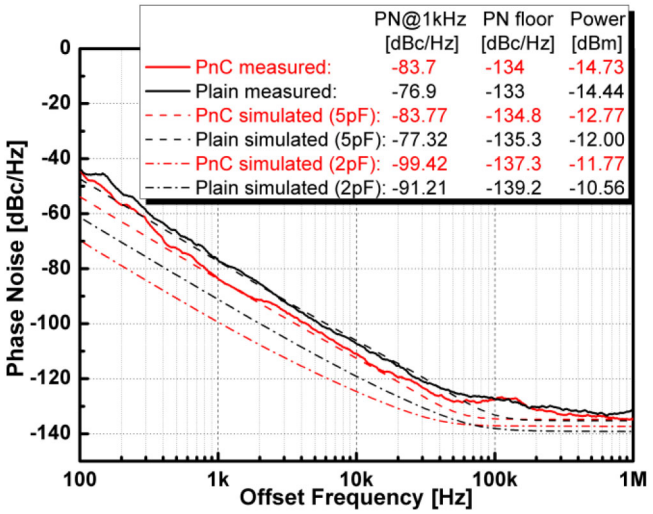

FIGURE 6. **Measured and simulated phase noise (PN) of the oscillators based on resonators with and without phononic crystal structures.**

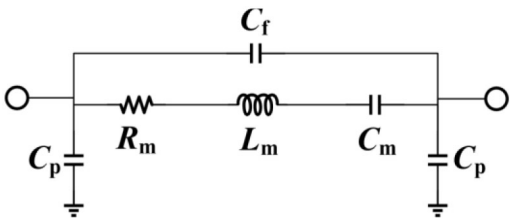

FIGURE 7. **Equivalent circuit model of the AlN-on-Si resonators adopted in the simulations.**

TABLE 1. **The extracted motional parameters of the AlN-on-Si MEMS resonators.**

Tether type	L_m [mH]	C_m [fF]	R_m [Ω]
Beam	0.515	2.476	171
Phononic Crystal	0.545	2.322	77

amplifier circuit in Advanced Design System (ADS) [16]. The equivalent circuit parameters (i.e., L_m, C_m and R_m) were determined from previous on-chip probing tests and listed in Table 1. The feedthrough capacitance (C_f) of the two-port AlN-on-Si resonator is usually very small (~10fF) and hardly affects the phase noise performance. The relatively large shunt capacitor (C_p), in the order of pF, in contrast has a notable negative impact on the phase noise performance according to our simulations. C_p here includes both the capacitance from the AlN-on-Si resonator structure (e.g., top Al electrode and bottom Si ground) and the parasitic capacitance from the wire bonds, which is difficult to quantify.

Fig. 6 presents the simulated phase noise of the oscillator with different C_p. The simulation captures the inherent flicker noise in the transimpedance amplifier as seen from a third order frequency roll off ($1/f^3$) phase noise slope in the close-to-carrier portion. Assuming C_p of about 5pF, the simulated phase noise matches the measured phase noise for both oscillators. Once C_p is reduced to 2pF, the simulation predicts a reduction of roughly 16dB in the close-to-carrier phase noise. As such, further phase noise improvement can be potentially achieved by cancelling out C_p [17]. Besides, given the level of the carrier power (below -14dBm), both AlN-on-Si resonators are working well below the nonlinear regime according to open loop measurements. Fig. 4b compares the measured and simulated time domain waveform of the oscillator output. It can be observed that the magnitude and shape of the simulated waveform agree well with our measured results, which further validates the use of the linear equivalent circuit model in the simulation.

TABLE 2. **Comparison of figure-of-merit with prior works.**

Reference	Noise at 1kHz [dBc/Hz]	f_0 [MHz]	P_{dc} [mW]	FOM [dB]	Mode
[18]	-81/-91	79/102	11.8/15.6	-88/-99	AlN Bulk
[19]	-88/-68	222/482	10	-105/-92	AlN Bulk
[20]	-82	427	13	-103	AlN-on-Si Bulk
[21]	-103	175	13.5	-116	AlN-on-Si Bulk
This work	-83	141	2.9	-101	AlN-on-Si Bulk

To facilitate a fair comparison with state-of-the-arts, we adopt a widely used figure-of-merit (FOM) [1] that involves normalizing the phase noise at 1kHz offset to a reference carrier frequency (10MHz) and reference dc power consumption (P_{dc}):

$$\text{FOM} = 10\log\left(L\,(1\text{kHz})\right) - 20\log\left(\frac{f_0\,[\text{MHz}]}{10\text{MHz}}\right) + 10\log\left(\frac{P_{dc}\,[\text{mW}]}{1\text{mW}}\right). \quad (4)$$

As shown in Table 2, the designed oscillator yields a figure-of-merit of -101dB at 1kHz offset, which is on par with state-of-the-art MEMS oscillators that combine AlN-based microresonators and CMOS sustaining circuitry. It is worth noting that our 65nm CMOS transimpedance amplifier is intended to lower P_{dc}, which in turn also limits the achievable carrier power. According to Eqn. (2), the phase noise floor can be further reduced by improving the transimpedance amplifier design to sustain higher carrier power.

IV. CONCLUSION

In this paper, we compared the phase noise performances of VHF MEMS-CMOS oscillators comprising AlN-on-Si MEMS resonators with different quality factors interfaced with a 65nm CMOS transimpedance amplifier. We have shown that using phononic crystal tethers engineered to boost the quality factor of the AlN-on-Si resonator for a specific frequency band results in a 6dB reduction in phase noise at 1kHz offset. Our work experimentally demonstrates that the addition of phononic crystal structures is a viable approach to reduce the close-to-carrier phase noise of MEMS oscillators based on low impedance AlN-on-Si resonators.

REFERENCES

[1] J. T. M. van Beek and R. Puers, "A review of MEMS oscillators for frequency reference and timing applications," *J. Micromech. Microeng.*, vol. 22, no. 1, Jan. 2012, Art. ID 013001.
[2] M. Lutz *et al.*, "MEMS oscillators for high volume commercial applications," in *Proc. TRANSDUCERS*, Lyon, France, Jun. 2007, pp. 49–52.
[3] M. Weinberg *et al.*, "Energy loss in MEMS resonators and the impact on inertial and RF devices," in *Proc. TRANSDUCERS*, Denver, CO, USA, Jun. 2009, pp. 688–695.
[4] A. Frangi, M. Cremonesi, A. Jaakkola, and T. Pensala, "Analysis of anchor and interface losses in piezoelectric MEMS resonators," *Sens. Actuat. A Phys.*, vol. 190, pp. 127–135, Feb. 2013.
[5] Z. Hao and B. Liao, "An analytical study on interfacial dissipation in piezoelectric rectangular block resonators with in-plane longitudinal-mode vibrations," *Sens. Actuat. A Phys.*, vol. 163, no. 1, pp. 401–409, Sep. 2010.
[6] R. Tabrizian and M. Rais-Zadeh, "The effect of charge redistribution on limiting the kt^2.Q product of piezoelectrically transduced resonators," in *Proc. TRANSDUCERS*, Anchorage, AK, USA, Jun. 2015, pp. 981–984.
[7] B. P. Harrington and R. Abdolvand, "In-plane acoustic reflectors for reducing effective anchor loss in lateral–extensional MEMS resonators," *J. Micromech. Microeng.*, vol. 21, no. 8, Aug. 2011, Art. ID 085021.
[8] C.-M. Lin, J.-C. Hsu, D. G. Senesky, and A. P. Pisano, "Anchor loss reduction in ALN lamb wave resonators using phononic crystal strip tethers," in *Proc. IEEE IFCS*, Taipei, Taiwan, May 2014, pp. 1–5.
[9] L. Sorenson, J. L. Fu, and F. Ayazi, "One-dimensional linear acoustic bandgap structures for performance enhancement of AlN-on-silicon micromechanical resonators," in *Tech Dig. Papers Transducers Conf.*, Beijing, China, Jun. 2011, pp. 918–921.
[10] H. Zhu and J. E.-Y. Lee, "AlN piezoelectric on silicon MEMS resonator with boosted Q using planar patterned phononic crystals on anchors," in *Proc. IEEE MEMS*, Estoril, Portugal, Jan. 2015, pp. 797–800.
[11] H. Zhu and J. E.-Y. Lee, "Design of phononic crystal tethers for frequency-selective quality factor enhancement in AlN piezoelectric-on-silicon resonators," in *Proc. Eurosensors Conf.*, Freiburg, Germany, Sep. 2015, pp. 516–519.
[12] Y.-W. Lin *et al.*, "Series-resonant VHF micromechanical resonator reference oscillators," *IEEE J. Solid-State Circuits*, vol. 39, no. 12, pp. 2477–2491, Dec. 2004.
[13] H. M. Lavasani, R. Abdolvand, and F. Ayazi, "A 500MHz low phase-noise A1N-on-silicon reference oscillator," in *Proc. IEEE CICC*, San Jose, CA, USA, Sep. 2007, pp. 599–602.
[14] D. Weinstein, H. Chandrahalim, L. F. Cheow, and S. A. Bhave, "Dielectrically transduced single-ended to differential MEMS filter," in *Tech. Dig. IEEE Int. Solid-State Circuits Conf.*, San Francisco, CA, USA, Feb. 2006, pp. 1236–1243.
[15] D. B. Leeson, "A simple model of feedback oscillator noise spectrum," *Proc. IEEE*, vol. 54, no. 2, pp. 329–330, Feb. 1966.
[16] *ADS Is a Registered Trademark of Keysight Technologies Inc.*, Santa Rosa, CA, USA. [Online]. Available: http://www.keysight.com/
[17] H. M. Lavasani, W. Pan, B. P. Harrington, R. Abdolvand, and F. Ayazi, "Electronic temperature compensation of lateral bulk acoustic resonator reference oscillators using enhanced series tuning technique," *IEEE J. Solid-State Circuits*, vol. 47, no. 6, pp. 1381–1393, Jun. 2012.
[18] K. E. Wojciechowski, R. H. Olsson, III, M. R. Tuck, E. Roherty-Osmun, and T. A. Hill, "Single-chip precision oscillators based on multi-frequency, high-Q aluminum nitride MEMS resonators," in *Proc. TRANSDUCERS*, Denver, CO, USA, Jun. 2009, pp. 2126–2130.
[19] C. Zuo, N. Sinha, J. Van der Spiegel, and G. Piazza, "Multifrequency pierce oscillators based on piezoelectric AlN contour-mode MEMS technology," *J. Microelectromech. Syst.*, vol. 19, no. 3, pp. 570–580, Jun. 2010.
[20] H. M. Lavasani, W. Pan, and F. Ayazi, "An electronically temperature-compensated 427MHz low phase-noise AlN-on-Si micromechanical reference oscillator," in *Proc. IEEE RFIC*, Anaheim, CA, USA, May 2010, pp. 329–332.
[21] H. M. Lavasani, R. Abdolvand, and F. Ayazi, "Single-resonator dual-frequency AIN-on-Si MEMS oscillators," *IEEE Trans. Ultrason., Ferroelectr., Freq. Control*, vol. 62, no. 5, pp. 802–813, May 2015.

PEI QIN was born in Sichuan, China. She received the B.S. degree in electronic science and technology from the University of Electronic Science and Technology of China, Chengdu, China, in 2010. She is currently pursuing the Ph.D. degree with the State Key Laboratory of Millimeter Waves, City University of Hong Kong. Her research interest includes radio frequency and millimeter wave integrated circuit design.

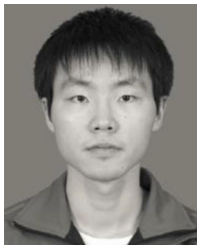

HAOSHEN ZHU (S'10) received the B.E. degree in electrical engineering from the Wuhan University of Technology, Wuhan, China, in 2009, and the Ph.D. degree in electronic engineering from the City University of Hong Kong, Hong Kong, in 2015.

He was a Senior Research Associate with the State Key Laboratory of Millimeter Waves, City University of Hong Kong. He is currently a Research Fellow with the University of Michigan, Ann Arbor, MI, USA. His research interests include micromechanical resonators, interface circuit design, and MEMS devices for timing and sensing applications.

Dr. Zhu was a recipient of the Student Award (in thematic: Materials, Resonators and Resonator Circuits) at the 28th European Frequency and Time Forum in 2014.

JOSHUA E.-Y. LEE (S'05–M'09) received the B.A. and M.Eng. degrees in 2005, and the Ph.D. degree in 2009, all from the University of Cambridge, U.K. He joined the Department of Electronic Engineering, City University of Hong Kong, in 2009, as a Faculty Member, where he is currently an Associate Professor and affiliated with the State Key Laboratory of Millimeter Waves. His research interests include the design, modeling, fabrication, and characterization of microelectromechanical systems (MEMS) structures and devices for sensing and frequency control, and studying issues arising from interfacing MEMS with circuits. He was a recipient of the Research Student Development Fellowship by the Royal Academy of Engineering, U.K., in 2008.

QUAN XUE (M'02–SM'04–F'11) received the B.S., M.S., and Ph.D. degrees in electronic engineering from the University of Electronic Science and Technology of China (UESTC), Chengdu, China, in 1988, 1990, and 1993, respectively.

In 1993, he joined the UESTC, as a Lecturer. He became a Professor in 1997. From 1997 to 1998, he was a Research Associate and then a Research Fellow with the Chinese University of Hong Kong. In 1999, he joined the City University of Hong Kong, where he is currently a Chair Professor of Microwave Engineering. He also serves as the Director of Information and Communication Technology Center, the Deputy Director of CityU Shenzhen Research Institute, and the Deputy Director of State Key Laboratory of Millimeter Waves, Hong Kong. He was the Associate Vice President with Innovation Advancement and China Office, from 2011 to 2015. He has authored or co-authored over 260 internationally referred journal papers and over 100 international conference papers. His research interests include microwave passive components, active components, antenna, microwave monolithic integrated circuits, and radio frequency integrated circuits.

Prof. Xue served the IEEE as an AdCom Member of MTT-S, from 2011 to 2013, and an Associate Editor of the IEEE TRANSACTIONS ON MICROWAVE THEORY AND TECHNIQUES from 2010 to 2013. Since 2010, he has been an Associate Editor of the IEEE TRANSACTIONS ON INDUSTRIAL ELECTRONICS.